LANGMUIR

pubs.acs.org/Langmuir Article

Universality in the Dynamics of Vesicle Translocation through a Hole

Bin Zheng, Fangfu Ye, Shigeyuki Komura,* and Masao Doi*

Cite This: *Langmuir* 2023, 39, 563−569 Read Online

ACCESS | Metrics & More | Article Recommendations

ABSTRACT: We analyze the translocation process of a spherical vesicle, made of a membrane and incompressible fluid, through a hole smaller than the vesicle size, driven by pressure difference ΔP. We show that such a vesicle shows certain universal characteristics, which are independent of the details of the membrane elasticity: (i) there is a critical pressure ΔP_c below which no translocation occurs; (ii) ΔP_c decreases to zero as the vesicle radius R_0 approaches the hole radius a, satisfying the scaling relation $\Delta P_c \sim (R_0 - a)^{3/2}$; and (iii) the translocation time τ diverges as ΔP decreases to ΔP_c, satisfying the scaling relation $\tau \sim (\Delta P - \Delta P_c)^{-1/2}$.

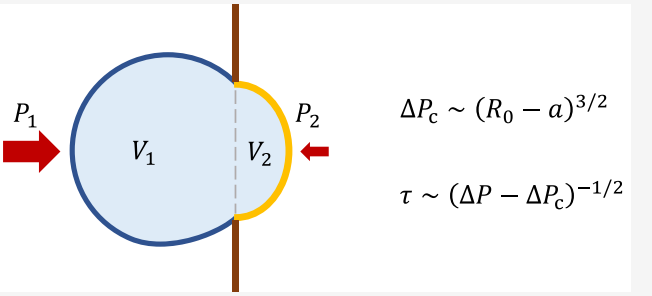

1. INTRODUCTION

A vesicle is a fluid droplet covered by a membrane. Vesicles play crucial roles in material transport in living systems. Artificial vesicles made of amphiphilic copolymers, called polymersomes, have been developed and are used as a capsule of drugs or RNA fragments.[1−5] Translocation of such objects through a constriction is ubiquitous in many biological and biotechnical systems, such as blood flow, cell circulation, drug delivery, and cell manufacturing.[6−12]

Many theoretical studies and simulations have been done for vesicle translocation,[13−18] but our understanding for these phenomena is still far from complete. One reason is that there exist many types of membranes (lipid membranes, polymer membranes, and cell membranes), and it is difficult to construct a general theory valid for all vesicles. Indeed, various models have been used in the past. In the early works,[13,18] it was assumed that the vesicles have a constant surface area but variable volume (as the fluid can permeate through the membrane). In recent works, alternative models have been used in which the vesicle has a constant volume but a variable surface area.[14,19,20] Another important difference is whether the membrane is a fluid, which has zero shear modulus in the plane, or an elastic sheet, which has a non-zero shear modulus.[21] In most of the previous works, the membrane has been assumed to be a fluid membrane, but an elastic membrane, often called the tethered membrane, exists and is important in many biological systems. Translocation of such membranes has been studied recently by computer simulations.[15]

In this work, we develop a theory for vesicle translocation using a model that can include a large class of membranes, such as fluid membranes, tethered membranes, and composite membranes. The model assumes that (i) the elastic energy of the membrane is due to the in-plane stretching of the membrane (i.e., the bending energy of the membrane is ignorable), (ii) the volume of the vesicle is kept constant during translocation (i.e., the fluid permeation through the membrane is ignorable), and (iii) the vesicle takes a spherical shape outside of the hole. We show that, if a vesicle satisfies these conditions, its translocation behavior has certain universal characteristics, which are independent of the details of the membrane property.

The outline of the article is as follows: In the Methods section, we discuss the general form of the free energy of a stretchable membrane model and give two specific models: (i) fluid membrane model and (ii) rubber membrane model. The time-evolution equation for the vesicle during translocation is derived. In the Results and Discussion section, we show the free energy profile for the translocation process and calculate the critical pressure needed to cause the translocation. We next show that there is certain universality in the critical pressure and the translocation time. We also summarize the assumptions used in our work and compare our main findings to previous simulation works. Finally, we conclude in the last section.

2. METHODS

2.1. General Membrane Model. We consider a spherical vesicle consisting of a membrane and inner fluid. The membrane can be a

Received: October 17, 2022
Revised: December 6, 2022
Published: December 22, 2022

https://doi.org/10.1021/acs.langmuir.2c02835
Langmuir 2023, 39, 563−569

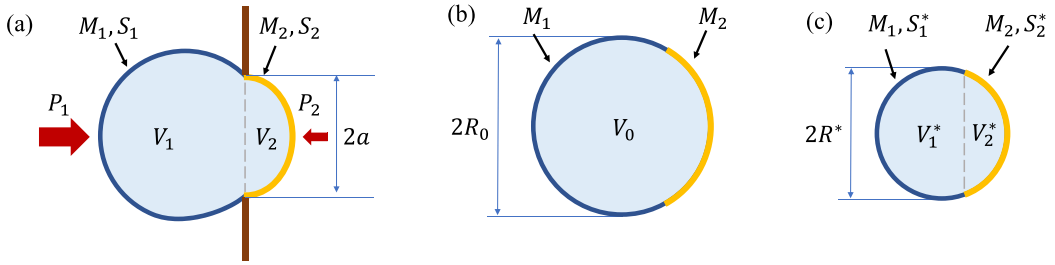

Figure 1. (a) When a vesicle is translocating through a hole of radius a, it takes a double spherical cap shape. The volume of the vesicle in each chamber is V_1 and V_2, and the area and mass of the membrane in each chamber are S_i and M_i (i = 1 and 2), respectively. (b) Outside of the hole, the vesicle takes a spherical shape of volume $V_0 = V_1 + V_2$. The parts of the membrane that are in chamber 1 or 2 in the state a are shown by different colors. (c) Vesicle in the reference state where the vesicle takes a spherical shape of radius R^*. The stretching λ_i of the membrane is defined by the length change with respect to this state. Notice that the volume V_0 in the state b is generally different from the volume $V^* = V_1^* + V_2^*$ in the state c.

single layer of amphiphilic molecules (uncross-linked or cross-linked polymers as in polymersomes) or composite membranes made of a fluid layer and elastic networks (as in plasma membranes).

We regard the membrane as a two-dimensional (2D) surface, described by a three-dimensional (3D) position vector $\mathbf{r}(s_1, s_2)$, where s_1 and s_2 are the 2D coordinates, which are defined in the reference state and identify a point in the membrane. We assume that, in the reference state, $\partial\mathbf{r}/\partial s_1$ and $\partial\mathbf{r}/\partial s_2$ are unit vectors orthogonal to each other [when we use the spherical coordinate (θ, ψ), s_1 and s_2 can be written as $s_1 = R^*\theta$ and $s_2 = (R^* \sin\theta)\psi$, where R^* is the radius of the sphere). We assume that the membrane is homogeneous and isotropic in the tangential plane. We also assume that the membrane is thin and ignore the bending energy. The elastic energy of the membrane is therefore due to the in-plane membrane stretching and can be characterized by the function $f(\lambda_1, \lambda_2)$, where λ_1 and λ_2 are the principal values of stretching and $f(\lambda_1, \lambda_2)$ is the elastic energy per unit area in the reference state [λ_1 and λ_2 are given by the square root of the eigenvalues of the 2 × 2 matrix $B_{ij} = (\partial\mathbf{r}/\partial s_i)\cdot(\partial\mathbf{r}/\partial s_j)$ with i and j = 1 and 2]. The total elastic energy functional of the membrane is given by the integral of $f(\lambda_1, \lambda_2)$ over the entire surface.

$$\mathcal{A}[\mathbf{r}(s_1, s_2)] = \int \mathrm{d}s_1\mathrm{d}s_2 f(\lambda_1, \lambda_2) \tag{1}$$

The equilibrium state of the membrane is calculated by minimizing this functional with respect to $\mathbf{r}(s_1, s_2)$.

For fluid membranes having zero 2D shear modulus, the free energy of the membrane depends upon the area per molecule, and therefore, $f(\lambda_1, \lambda_2)$ depends only upon the area change ratio $\lambda_1\lambda_2$. In this work, we consider the following model energy:

$$f_{\mathrm{FM}}(\lambda_1, \lambda_2) = \frac{k_a}{2}(\lambda_1\lambda_2 - 1)^2 \tag{2}$$

where k_a is the elastic constant, which has the same dimension as the surface tension.

For elastic (or tethered) membranes, f cannot be written in the form of eq 2 because they experience restoring force caused by shear strain $\lambda_1 - \lambda_2$. As an example, we consider the following neo-Hookean model,[22] which has been extensively used as a model of a rubber membrane (such as balloons):

$$f_{\mathrm{RM}}(\lambda_1, \lambda_2) = \frac{\mu d}{2}[\lambda_1^2 + \lambda_2^2 + (\lambda_1\lambda_2)^{-2} - 3] \tag{3}$$

where μ is the 3D shear modulus of the rubber and d is the thickness of the membrane. We call such a membrane a rubber membrane.

2.2. Free Energy of a Vesicle under Translocation. We now consider the situation that such a vesicle is forced to pass through a hole of radius a made in a wall at the boundary between two chambers 1 and 2, as shown in Figure 1. Initially, the vesicle has a spherical shape of radius R^* (Figure 1c), and it is inflated to have a radius R_0 by some methods (e.g., osmotic swelling or injection) (Figure 1b). We use the swelling ratio defined by $\eta = R_0/R^* \geq 1$. The pressure in each chamber is P_1 and P_2, and the vesicle is pushed by the pressure difference $\Delta P = P_1 - P_2 > 0$. During the translocation, the vesicle takes a double spherical cap shape, each having volume V_1 and V_2 (Figure 1a). Because the membrane is assumed to be impermeable to the fluid during the passage, the total fluid volume $V_0 = V_1 + V_2 = 4\pi R_0^3/3$ remains unchanged. Let S_1 and S_2 be the areas of the membrane in each chamber. Because the membrane can be stretched, the total area of the membrane $S = S_1 + S_2$ can vary. To describe the transport of the membrane, we introduce the membrane mass M_1 and M_2 in each chamber. The total mass $M_0 = M_1 + M_2$ remains constant, but the membrane mass density M_i/S_i (i = 1 and 2) in each chamber changes in time.

Given the free energy functional, such as eq 1, the free energy of the vesicle is uniquely determined as a function of M_i and V_i and is written as

$$G = A(M_1, V_1) + A(M_2, V_2) + P_1V_1 + P_2V_2 \tag{4}$$

where $A(M_i, V_i)$ is the minimum of the functional $\mathcal{A}[\mathbf{r}(s_1, s_2)]$ subject to the constraint that the membrane has mass M_i and includes fluid volume V_i and that its circular edge is fixed to the hole of radius a. In eq 4, contributions from the internal pressure P_{int} of the vesicles, written as $P_{\mathrm{int}}(V_1 + V_2)$, are eliminated as a result of the constant $V_0 = V_1 + V_2$. In the following, we calculate $A(M_i, V_i)$ explicitly for a fluid membrane and a rubber membrane.

2.2.1. Fluid Membrane. We first consider the fluid membrane model. The fluid membrane at equilibrium always takes a spherical cap shape with a constant curvature. Therefore, the area change ratio $\lambda_1\lambda_2$ in eq 2 is equal to S_i/S_i^* in each chamber, and the integral of eq 2 can be written as $S_i^* f(S_i/S_i^*)$. The total free energy can be written as

$$G(M_i, V_i) = \frac{k_a}{2}\frac{[S_1(V_1) - S_1^*(M_1)]^2}{S_1^*(M_1)} + \frac{k_a}{2}\frac{[S_2(V_2) - S_2^*(M_2)]^2}{S_2^*(M_2)} + P_1V_1 + P_2V_2 \tag{5}$$

where $S_i^* = 4\pi(R^*)^2 M_i/M_0$ is the area of the membrane of mass M_i in the reference state (Figure 1c). The surface area S_i is determined by the condition that the spherical cap has volume V_i and its edge is fixed to a circle of radius a. This condition leads to $S_i = \pi(a^2 + h_i^2)$, where h_i is the solution of the equation $V_i = \pi h_i(3a^2 + h_i^2)/6$ for given V_i. Therefore, the energy of the fluid membrane can be expressed in terms of M_i and V_i.

Because $V_0 = V_1 + V_2$ and $M_0 = M_1 + M_2$ are constant, the total free energy G can be expressed as a function of V_2 and M_2. We define the following dimensionless quantities:

$$x = \frac{M_2}{M_0} - \frac{1}{2}, \quad y = \frac{V_2}{V_0} - \frac{1}{2} \tag{6}$$

and write the total free energy as

https://doi.org/10.1021/acs.langmuir.2c02835
Langmuir 2023, 39, 563−569

$$G(x, y) = \frac{k_a}{2}\frac{[S_1(y) - (1/2 - x)S^*]^2}{(1/2 - x)S^*} + \frac{k_a}{2}\frac{[S_2(y) - (1/2 + x)S^*]^2}{(1/2 + x)S^*} - \Delta P V_0 y \quad (7)$$

where $S^* = S_0/\eta^2$ and $\eta = R_0/R^*$ is the swelling ratio. In addition, S_2/S_0 can be derived from the geometric relation for a spherical cap, as mentioned above, and becomes

$$\frac{S_2(y, a/R_0)}{S_0} = -\frac{(a/R_0)^2}{4} + \frac{(a/R_0)^4}{4\beta^{2/3}} + \frac{\beta^{2/3}}{4} \quad (8)$$

where

$$\beta(y, a/R_0) = 4(y + 1/2) + \sqrt{(a/R_0)^6 + 16(y + 1/2)^2} \quad (9)$$

Similarly, $S_1(y, a/R_0)/S_0$ is obtained by replacing y with $-y$ in the above equation.

2.2.2. Rubber Membrane. We next consider the rubber membrane whose free energy is given by eq 3. To calculate the elastic free energy, we first focus on the spherical cap in chamber 2, which has the surface mass M_2 and is initially a part of the equilibrium vesicle of radius R^*. Then, it is fixed to the hole of radius a and is inflated to the volume V_2, as shown by the yellow curve in Figure 1a.

Exact calculation of the elastic energy for such deformation is difficult for a rubber membrane. Here, we use an approximation and assume that the membrane takes a spherical shape of curvature $1/R_2$, as shown in Figure 2. Then, a point located at a polar angle θ on the

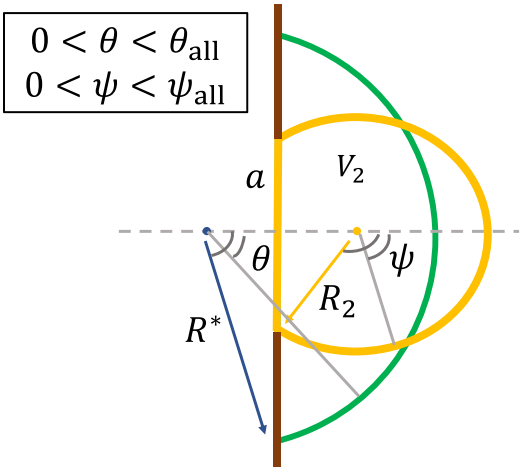

Figure 2. Schematic illustration of the rubber membrane model.

sphere of radius R^* in the reference state will move to a point located at a polar angle $\psi(\theta)$ on the inflated sphere of radius R_2. This deformation elongates the line segment along the θ direction by factor $R_2 d\psi/R^* d\theta$ and the line segment perpendicular to this direction by factor $R_2 \sin\psi/R^* \sin\theta$. Hence, the principal values of stretching in chamber 2 are given by

$$\lambda_{21} = \frac{R_2}{R^*}\frac{d\psi}{d\theta}, \quad \lambda_{22} = \frac{R_2 \sin\psi}{R^* \sin\theta} \quad (10)$$

To determine the functional form of $\psi(\theta)$, we assume that the surface area of the membrane changes uniformly by deformation, such that $\lambda_{21}\lambda_{22}$ is constant (independent of θ). This condition gives

$$\frac{\sin\psi}{\sin\theta}\frac{d\psi}{d\theta} = \text{constant} \quad (11)$$

From this relation, we have

$$\frac{1 - \cos\theta}{1 - \cos\psi} = \frac{1 - \cos\theta_{all}}{1 - \cos\psi_{all}} \quad (12)$$

where θ_{all} and ψ_{all} are the maximum values of θ and ψ, respectively, which are given by (see Figure 2)

$$\theta_{all} = \arccos(-2x) \quad (13)$$

$$\psi_{all} = \arccos\left[1 - \frac{2S_2/S_0}{(R_2/R_0)^2}\right] \quad (14)$$

Here, $R_2(y)/R_0$ can be derived from the geometric relation for a spherical cap, $S_2 = 2\pi R_2 h_2$, where h_2 is the solution of the equation $V_2 = \pi h_2^2(3R_2 - h_2)/3$. On the other hand, $S_2(y, a/R_0)/S_0$ is given by eqs 8 and 9. Then, the same calculation can be done for the membrane in chamber 1.

The total energy of deformation can be expressed by the integrals over θ

$$G(x, y) = \frac{\mu d}{2}\int_0^{\pi-\theta_{all}} d\theta\left(\lambda_{11}^2 + \lambda_{12}^2 + \frac{1}{\lambda_{11}^2\lambda_{12}^2} - 3\right) \times 2\pi(R^*)^2 \sin\theta + \frac{\mu d}{2}\int_0^{\theta_{all}} d\theta\left(\lambda_{21}^2 + \lambda_{22}^2 + \frac{1}{\lambda_{21}^2\lambda_{22}^2} - 3\right) \times 2\pi(R^*)^2 \sin\theta - \Delta P V_0 y \quad (15)$$

Although the above integrals can be performed analytically, it is too lengthy to present the result here.

2.3. Time-Evolution Equation. If the free energy of the system is expressed as a function of x and y, the time evolution can be discussed in the same way as in the previous works.[20] Here, it is important to note that the characteristic times of x and y are quite different from each other. The membrane mass transport is governed by the solid friction of the membrane sliding against the hole, while the fluid volume transport is governed by the fluid flow through the hole. Because the fluid friction is much smaller than the solid friction, the relaxation time of y is much smaller than that of x. Therefore, we may assume that y is at equilibrium for a given value of x. Hence, y is determined by the condition

$$\frac{\partial G(x, y)}{\partial y} = 0 \quad (16)$$

Let $y = y^*(x)$ be the solution of this equation. The total free energy is therefore written as a function of x only, and we write it as

$$G_x^* = G(x, y^*(x)) \quad (17)$$

Then, the time-evolution equation for x is written as

$$\xi(x)\frac{dx}{dt} = -\frac{dG_x^*}{dx} \quad (18)$$

where $\xi(x)$ is the friction coefficient representing the solid friction for the membrane sliding at the hole rim.

3. RESULTS AND DISCUSSION

3.1. Free Energy Profile. Figure 3 shows an example of G_x^* calculated for a fluid membrane whose free energy is given by eq 7. When there is no pressure difference, i.e., when $\Delta P = 0$, G_x^* has a peak at $x = 0$. When a small pressure is applied, G_x^* has a local minimum in the region of $x < 0$. This corresponds to the situation that the vesicle is trapped by the hole. By the further increase of ΔP, the local minimum becomes unstable (see the curve of $\Delta P R_0/k_a \approx 0.18$ in Figure 3). The vesicle translocates from chamber 1 to 2 above this critical pressure difference.

3.2. Critical Pressure for Translocation. The above argument shows that the critical pressure difference ΔP_c is determined by the following condition for general membranes

$$\frac{dG_x^*}{dx} = \frac{d^2G_x^*}{dx^2} = 0 \quad (19)$$

https://doi.org/10.1021/acs.langmuir.2c02835
Langmuir 2023, 39, 563−569

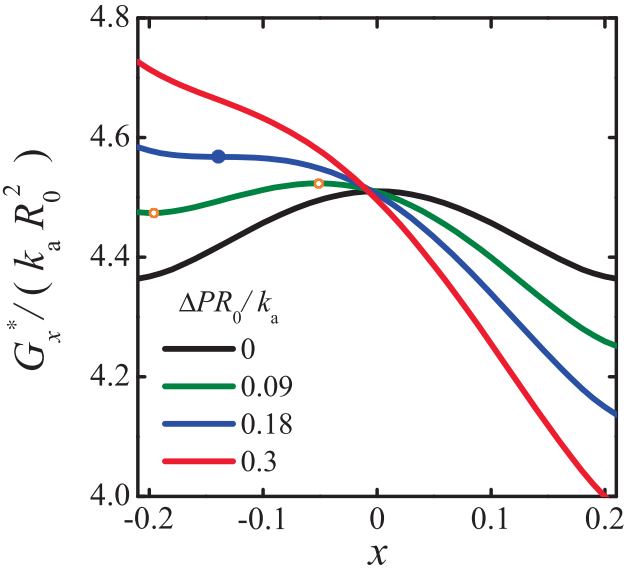

Figure 3. Free energy G_x^* of a fluid membrane as a function of $x = M_2/M_0 - 1/2$ when $a/R_0 = 0.9$ for different values of ΔP.

Although ΔP_c can be obtained by solving eq 19, the calculation becomes somewhat cumbersome. However, there is a simpler way of calculating ΔP_c.

We consider the function $G_y^* = G(x^*(y), y)$, where $x^*(y)$ is the solution of $\partial G(x, y)/\partial x = 0$. In Appendix A, we show that the critical state can also be obtained by solving the following equation:

$$\frac{dG_y^*}{dy} = \frac{d^2G_y^*}{dy^2} = 0 \tag{20}$$

The advantage of using G_y^* is that $x^*(y)$ is independent of ΔP and satisfies the symmetry relation $x^*(-y) = -x^*(y)$. Hence, G_y^* can be written in the following form:

$$G_y^* = A_{tot}(y) - \Delta P V_0 y \tag{21}$$

where $A_{tot}(y)$ stands for the minimum of the total membrane elastic energy [i.e., $A_{tot}(y) = \min(A(M_1, V_1) + A(M_2, V_2)]$ subject to the constraint that the inner fluid volume in chamber 2 is $(1/2 + y)V_0$. Notice that $A_{tot}(y)$ satisfies the relation $A_{tot}(-y) = A_{tot}(y)$.

Further simplification is possible for fluid membranes for which $A(M_i, V_i)$ can be written as $S_i^* f(S_i/S_i^*)$. Then, the condition $\partial G(x, y)/\partial x = 0$ gives the relation $S_1/S_1^* = S_2/S_2^* = S/S^*$, where $S = S_1 + S_2$ is the total surface area of the vesicle and $S^* = S_0/\eta^2$. The free energy G_y^* can be written as

$$\begin{aligned} G_y^* &= S_1^* f(S_1/S_1^*) + S_2^* f(S_2/S_2^*) - \Delta P V_0 y \\ &= S^* f(S/S^*) - \Delta P V_0 y \end{aligned} \tag{22}$$

For given a and R_0, S depends only upon y. For eq 22, the first equation in eq 20 gives the following equilibrium pressure ΔP at state y:

$$\Delta P = \frac{f'}{V_0}\frac{dS}{dy} \tag{23}$$

The second equation in eq 20 gives the following equation for y_c at the critical state:

$$\frac{f''}{S^*}\left(\frac{dS}{dy}\right)^2 + f'\frac{d^2S}{dy^2} = 0 \tag{24}$$

where f' and f'' stand for the first and second derivatives of the function f, respectively. In addition, S/S_0 is derived from the geometric relation for a spherical cap and is given by eqs 8 and 9. Finally, the analytical expression of ΔP in eq 23 can be obtained, but it is too lengthy to present it here.

In Figure 4a, we plot ΔP_c of the fluid membrane described by eq 2 when $\eta = R_0/R^* = 1.5$. Naturally, ΔP_c approaches zero

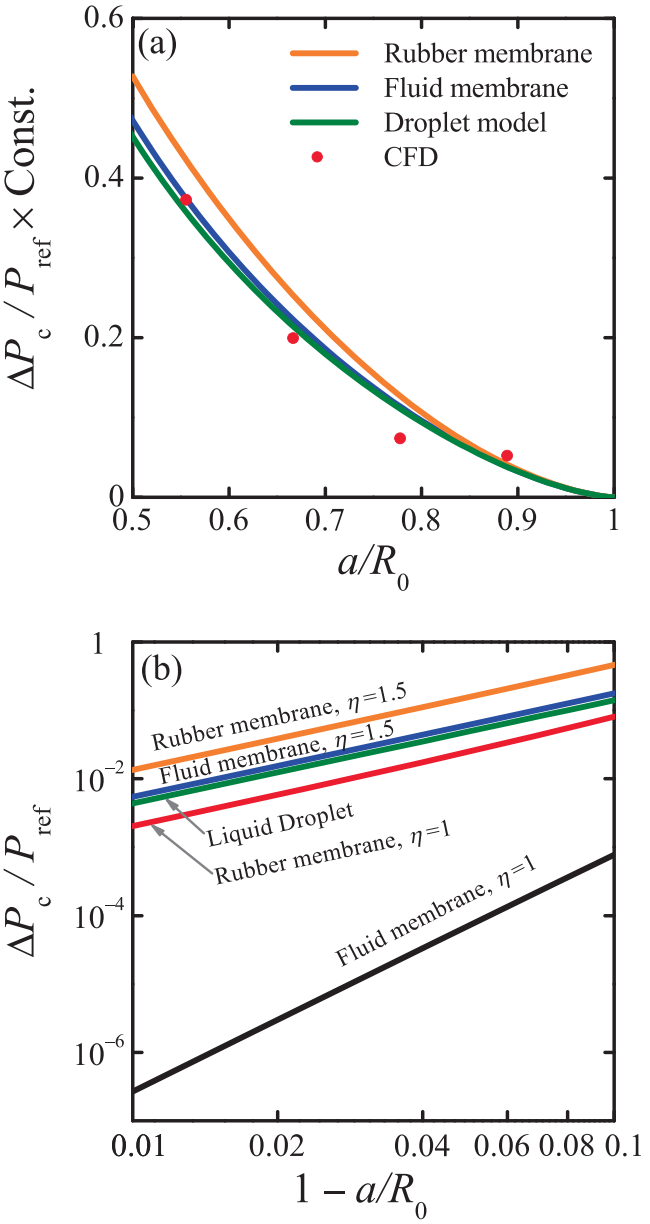

Figure 4. (a) Reduced critical pressure $\Delta P_c/P_{ref}$ as a function of a/R_0 for different membrane models when $\eta = R_0/R^* = 1.5$. Here, P_{ref} corresponds to k_a/R_0 for a fluid membrane, $\mu d/R_0$ for a rubber membrane, and γ/R_0 for a liquid droplet, respectively. The constant factors in $\Delta P_c/P_{ref}$ are chosen to have an overlap of different curves when a/R_0 is close to unity. The red circles are the data obtained by the computational fluid dynamics (CFD) in ref 10. (b) Double-logarithmic plot of panel a as a function of $1 - a/R_0$ for different membrane models when $\eta = 1.5$ and 1.

https://doi.org/10.1021/acs.langmuir.2c02835
Langmuir 2023, 39, 563−569

for $a/R_0 \to 1$. In Figure 4b, we show the dependence of ΔP_c on $1 - a/R_0$ in the double-logarithmic plot. The plot indicates the scaling relation $\Delta P_c \sim (1 - a/R_0)^{\alpha}$. The exponent is $\alpha = {}^3/_2$ for most cases, whereas the only exception is the case of $\eta = 1$ (unswollen vesicle), for which we have $\alpha = {}^7/_2$.

Further analytical calculation of ΔP_c is possible when $\varepsilon_a = 1 - a/R_0$ is small. For $\varepsilon_a \ll 1$, we obtain

$$\Delta P_c \approx \frac{16\sqrt{6}}{9}\frac{k_a}{R_0}\frac{[(\eta^2 - 1)\varepsilon_a + (10 - 7\eta^2)\varepsilon_a{}^3/3]^{3/2}}{[(\eta^2 - 1) + 3(5 - 4\eta^2)\varepsilon_a{}^2]^{1/2}} \tag{25}$$

This expression explicitly shows that, apart from the special case of $\eta = 1$, the exponent is $\alpha = {}^3/_2$. In the limit of $\eta \gg 1$, the critical pressure becomes

$$\Delta P_c \approx \frac{16\sqrt{6}}{9}\frac{\gamma}{R_0}\varepsilon_a{}^{3/2} \tag{26}$$

where $\gamma = \eta^2 k_a$ is the effective surface tension of the vesicle at the initial state. In the limit of $\eta \gg 1$, the area change of the vesicle during translocation is small and the vesicle can be regarded as a liquid droplet (without any membrane), having the constant surface tension γ.[23] Indeed, the same result can be obtained from the analysis of a liquid droplet whose shape is controlled only by surface tension, as shown in Appendix B.

3.3. Universality in the Critical Pressure. We have shown that the critical pressure approaches zero as the hole size approaches the equilibrium vesicle size according to the scaling relation $\Delta P_c \propto (1 - a/R_0)^{3/2}$. We now show that, apart from the exceptional case, the exponent $\alpha = {}^3/_2$ is always valid for spherical vesicles (for both fluid and elastic membranes) as long as the free energy is written in the form of eq 4.

We start from the expression for the free energy in eq 21 that is valid for $|y|$ less than a certain value $y_m > 0$. This range of y becomes smaller as ε_a becomes smaller. Therefore, we may expand $A_{tot}(y)$ with respect to y. Because $A_{tot}(y)$ is an even function of y, $G_y{}^*$ can be written as

$$G_y{}^* \approx -\Delta P V_0 y - B_1 y^2 + B_2 y^4 + \ldots \tag{27}$$

The coefficients B_1 and B_2 depend upon the vesicle properties (e.g., size and elasticity) and also the hole size a. For small $\Delta P > 0$, $G_y{}^*$ has a local minimum at a certain value of y that satisfies $-y_m < y < 0$. As ΔP increases, the local minimum disappears and $G_y{}^*$ becomes a monotonically decreasing function of y. For $G_y{}^*$ to have such a shape change, both B_1 and B_2 must be positive, whereas the coefficient B_1 has to vanish as $\varepsilon_a \to 0$. Hence, we may assume $B_1 = b_1\varepsilon_a$, where b_1 is a positive constant. Then, eqs 20 and 27 give the following critical state:

$$y_c = -\left(\frac{b_1\varepsilon_a}{6B_2}\right)^{1/2}, \qquad \Delta P_c = \frac{2\sqrt{6}\, b_1{}^{3/2}\varepsilon_a{}^{3/2}}{9V_0 B_2{}^{1/2}} \tag{28}$$

The latter result shows that the relation $\Delta P_c \sim \varepsilon_a{}^{3/2}$ holds generally and is independent of the detail of the membrane property.

The singular behavior for a fluid membrane when $\eta = 1$ (black line in Figure 4b) arises from the fact that b_1 in the above argument vanishes. If the vesicle is swollen ($\eta > 1$) or if the membrane is tethered, b_1 becomes non-zero and the exponent $\alpha = {}^3/_2$ is recovered. To demonstrate this, we calculate ΔP_c for a rubber membrane with eq 15, and the result is shown in Figure 4b. For the rubber membrane, we see that the exponent α does not show any singularity at $\eta = 1$, as shown by the orange and red lines in Figure 4b.

3.4. Universality in the Translocation Time. Finally, we consider the vesicle translocation time τ, i.e., the time needed for the vesicle to pass through the hole. It can be calculated by integrating $(dx/dt)^{-1}$ in eq 18 from the initial value to the final value

$$\tau = \int_{-x_m}^{x_m} dx \xi(x)\left(-\frac{dG_x{}^*}{dx}\right)^{-1} \tag{29}$$

where x_m defines the range of the integration. The translocation time τ diverges as ΔP approaches ΔP_c. The relation between τ and $\Delta P - \Delta P_c$ can be obtained by the similar phenomenological argument as before.

We consider the situation that ΔP is slightly larger than ΔP_c. We define a dimensionless parameter $\varepsilon_P = \Delta P/\Delta P_c - 1 > 0$, which is small in the current situation. Then, the translocation time is essentially determined by the time needed for the vesicle to pass through the small region near the critical point x_c. In such a case, the friction coefficient $\xi(x)$ can be replaced by a constant $\xi_c = \xi(x_c)$ and the derivative of $G_x{}^*$ can be expanded in terms of $x - x_c$ as

$$-\frac{dG_x{}^*}{dx} = C_0 + C_1(x - x_c) + C_2(x - x_c)^2 + \ldots \tag{30}$$

where the coefficients C_i ($i = 0, 1, 2, \ldots$) are functions of ε_P. The condition for the critical state in eq 19 imposes that C_0 and C_1 must vanish when $\varepsilon_P = 0$. We may thus assume $C_0 = c_0\varepsilon_P$ and $C_1 = c_1\varepsilon_P$. In the limit of $\varepsilon_P \to 0$, the integral becomes independent of x_m and c_1 and approaches the following asymptotic value:

$$\tau \approx \int_{-\infty}^{\infty} dx \frac{\xi_c}{c_0\varepsilon_P + C_2(x - x_c)^2} = \frac{\pi\xi_c\varepsilon_P{}^{-1/2}}{(c_0 C_2)^{1/2}} \tag{31}$$

Therefore, the translocation time is proportional to $\varepsilon_P{}^{-1/2}$ or $(\Delta P - \Delta P_c)^{-1/2}$, which is another universal property of the vesicle translocation.

3.5. Basic Assumptions. We have shown that the translocation dynamics of vesicles has certain universal properties, which are independent of the detail of the membranes. We now discuss the base of the assumptions used to derive these properties. There are two important assumptions: (i) The vesicle is a sphere in free space and takes a spherical cap shape on both sides of the hole, and its total volume is kept constant during translocation. (ii) The bending energy of the membrane is ignorable.

The first assumption is justified for a fluid membrane, but it is an approximation for an elastic membrane. This assumption will hold if the vesicle is inflated and the membrane is subject to tension, but it will not hold for a deflated vesicle or a vesicle that has wrinkles. The second assumption is different from previous works. We did not use the Helfrich model[24] that is widely used for lipid membranes because our aim is to study the effect of membrane stretching. If the 2D area of the membrane changes, its energy is much larger than the bending energy because the Föpl von Kármán number (the ratio between the stretching energy and the bending energy) $(R_0/h)^2$ (h being the thickness of the membrane) is much larger than unity.

There are other assumptions that are introduced to make the theory simple, such as (iii) the thickness of the hole is

https://doi.org/10.1021/acs.langmuir.2c02835
Langmuir 2023, 39, 563−569

ignorable and (iv) the adhesion between the membrane and the wall around the hole is ignorable. These assumptions can be removed, and the ignored effects can be included in the same way as the previous works[14,19] but do not affect the scaling relation proposed in this paper.

3.6. Comparison to Other Works. Thus far, there are scarce data (experimental or simulation) to be compared to our predictions. The critical pressure for a droplet passing through a channel was studied by numerically solving the hydrodynamic equations,[10] and they are plotted by the red circles in Figure 4a. Furthermore, we give a simple estimation of ΔP_c using eq 25. In the experiment, the typical radius of a polymersome is $R_0 \approx 20\ \mu$m, and its stretching modulus is $k_a \approx 0.1$ N/m^3. Considering $a/R_0 = 0.8$ and $\eta = 2$, we obtain $\Delta P_c \approx 3 \times 10^3$ Pa, which is consistent with the above work.[10]

Other work to be compared is the molecular dynamics simulation for the translocation of tethered vesicles by Ranguelov et al.[15] They reported the existence of ΔP_c and studied the exponent ω, which describes the divergence of the translocation time as $\tau \sim (\Delta P - \Delta P_c)^{-\omega}$. They found that ω varies from 0.22 to 0.85 depending upon the hole size. Although our theory is not in contradiction with their results, the reason for the deviation needs to be studied.

4. CONCLUSION

We have shown that there is a universality in the translocation of a wide class of vesicles that take spherical shapes in the free state: (i) there is a critical pressure difference ΔP_c for the translocation to take place; (ii) the critical pressure obeys the scaling relation $\Delta P_c \sim (R_0 - a)^{3/2}$; and (iii) the translocation time diverges as $\tau \sim (\Delta P - \Delta P_c)^{-1/2}$. We have shown that they are in agreement with rigorous calculations for fluid membranes and an approximate calculation for rubber membranes. More studies are needed to confirm the validity of the present theory. Finally, we hope that the universality as shown in our theory will provide insight into the applications of the vesicle translocation in living systems.

APPENDIX A

Proof of Equivalence of the Two Ways in Determining Critical Points

We consider a free energy function $G(x, y, P)$, which has two independent variables x and y and includes a parameter P. The equilibrium state is given by

$$\frac{\partial G}{\partial x} = 0, \quad \frac{\partial G}{\partial y} = 0 \tag{A1}$$

Suppose that the above local minimum becomes unstable at a certain critical value P_c. It can be obtained in two ways:

(i) P_c is obtained by solving the following set of equations:

$$\frac{\partial G}{\partial x} = 0, \quad \frac{\partial G}{\partial y} = 0, \quad \frac{\partial^2 G}{\partial x^2}\frac{\partial^2 G}{\partial y^2} - \left(\frac{\partial^2 G}{\partial x \partial y}\right)^2 = 0 \tag{A2}$$

The first two equations indicate that $G(x, y)$ becomes stationary at (x_c, y_c), and the third equation indicates that the same stationary state is at the stability limit.

(ii) We reduce the two-variable function $G(x, y)$ to a one-variable function

$$G_x^* = \min_y G(x, y) = G(x, y^*(x)) \tag{A3}$$

where $y^*(x)$ is the solution of $\partial G/\partial y = 0$. Then, P_c is obtained by the condition that the local minimum of G_x^* becomes unstable at P_c.

$$\frac{dG_x^*}{dx} = 0, \quad \frac{d^2 G_x^*}{dx^2} = 0 \tag{A4}$$

These two methods are equivalent and give the same value for P_c. This is proven as follows:

We use the formula

$$\frac{dG(x, y^*(x))}{dx} = \frac{\partial G}{\partial x} + \frac{\partial G}{\partial y}\frac{dy^*}{dx} \tag{A5}$$

Then, using the relation $\partial G(x, y^*)/\partial y = 0$, we obtain

$$\frac{dG_x^*}{dx} = \frac{\partial G}{\partial x} + \frac{\partial G}{\partial y}\frac{dy^*}{dx} = \frac{\partial G(x, y^*)}{\partial x} \tag{A6}$$

Using eq A5, we have

$$\frac{d^2 G_x^*}{dx^2} = \frac{\partial^2 G}{\partial x^2} + \frac{\partial^2 G}{\partial x \partial y}\frac{dy^*}{dx} \tag{A7}$$

On the other hand, because $\partial G(x, y^*)/\partial y = 0$, we have

$$\frac{d}{dx}\left(\frac{\partial G(x, y^*)}{\partial y}\right) = \frac{\partial^2 G}{\partial y \partial x} + \frac{\partial^2 G}{\partial y^2}\frac{dy^*}{dx} = 0 \tag{A8}$$

Therefore, $dy^*/dx = -(\partial^2 G/\partial x \partial y)/(\partial^2 G/\partial y^2)$. Hence, the second condition in eq A4 is written as

$$\frac{d^2 G_x^*}{dx^2} = \frac{\partial^2 G}{\partial x^2} - \frac{\left(\frac{\partial^2 G}{\partial x \partial y}\right)^2}{\frac{\partial^2 G}{\partial y^2}} = \frac{\frac{\partial^2 G}{\partial x^2}\frac{\partial^2 G}{\partial y^2} - \left(\frac{\partial^2 G}{\partial x \partial y}\right)^2}{\frac{\partial^2 G}{\partial y^2}} = 0 \tag{A9}$$

This condition is equivalent to eq A2. Similarly, we can prove the equivalence using the variable y.

$$\frac{d^2 G_y^*}{dy^2} = \frac{\partial^2 G}{\partial y^2} - \frac{\left(\frac{\partial^2 G}{\partial x \partial y}\right)^2}{\frac{\partial^2 G}{\partial x^2}} = \frac{\frac{\partial^2 G}{\partial x^2}\frac{\partial^2 G}{\partial y^2} - \left(\frac{\partial^2 G}{\partial x \partial y}\right)^2}{\frac{\partial^2 G}{\partial x^2}} = 0 \tag{A10}$$

APPENDIX B

Derivation of the Liquid Droplet Case

The free energy G for the case of the liquid droplet surface has the following form:

$$G(y) = \gamma S_1(y) + \gamma S_2(y) - \Delta P V_0 y \tag{B1}$$

where $y = V_2/V_0 - 1/2$ and $S_i(y)$ can be obtained from eqs 8 and 9. Minimizing $G(y)$ with respect to y, we obtain

$$\Delta P(y, a, \eta) = \frac{3\gamma}{R_0}\left(\frac{dS_1/S_0}{dy} + \frac{dS_2/S_0}{dy}\right) \tag{B2}$$

By taking the same strategy as the fluid membrane case, the analytical expression of ΔP_c is given as

$$\Delta P_c \approx \frac{16\sqrt{6}\,\gamma \epsilon_a^{3/2}}{9R_0} \tag{B3}$$

https://doi.org/10.1021/acs.langmuir.2c02835
Langmuir 2023, 39, 563−569

AUTHOR INFORMATION

Corresponding Authors

Shigeyuki Komura − *Wenzhou Institute, University of Chinese Academy of Sciences, Wenzhou, Zhejiang 325001, People's Republic of China; Oujiang Laboratory, Wenzhou, Zhejiang 325000, People's Republic of China; Department of Chemistry, Graduate School of Science, Tokyo Metropolitan University, Tokyo 192-0397, Japan;* orcid.org/0000-0003-3422-5745; Email: komura@wiucas.ac.cn

Masao Doi − *Wenzhou Institute, University of Chinese Academy of Sciences, Wenzhou, Zhejiang 325001, People's Republic of China; Oujiang Laboratory, Wenzhou, Zhejiang 325000, People's Republic of China*; Email: doi.masao@a.mbox.nagoya-u.ac.jp

Authors

Bin Zheng − *Wenzhou Institute, University of Chinese Academy of Sciences, Wenzhou, Zhejiang 325001, People's Republic of China; Oujiang Laboratory, Wenzhou, Zhejiang 325000, People's Republic of China;* orcid.org/0000-0003-2636-4120

Fangfu Ye − *Wenzhou Institute, University of Chinese Academy of Sciences, Wenzhou, Zhejiang 325001, People's Republic of China; Oujiang Laboratory, Wenzhou, Zhejiang 325000, People's Republic of China; School of Physical Science, University of Chinese Academy of Sciences, Beijing 100049, People's Republic of China; Beijing National Laboratory for Condensed Matter Physics, Institute of Physics, Chinese Academy of Sciences, Beijing 100190, People's Republic of China;* orcid.org/0000-0003-1279-105X

Complete contact information is available at: https://pubs.acs.org/10.1021/acs.langmuir.2c02835

Notes

The authors declare no competing financial interest.

ACKNOWLEDGMENTS

Bin Zheng, Shigeyuki Komura, and Masao Doi acknowledge the startup fund of Wenzhou Institute, University of Chinese Academy of Sciences (WIUCASQD2022016, WIUCASQD2021041, and WIUCASQD2022004) and Oujiang Laboratory (OJQDSP2022018). Bin Zheng and Shigeyuki Komura acknowledge the National Natural Science Foundation of China (NSFC) through Grants 22203022, 12274098, and 12250710127.

REFERENCES

(1) Lee, J. S.; Feijen, J. Polymersomes for drug delivery: Design, formation and characterization. *J. Controlled Release* **2012**, *161*, 473−483.

(2) Rideau, E.; Dimova, R.; Schwille, P.; Wurm, F. R.; Landfester, K. Liposomes and polymersomes: A comparative review towards cell mimicking. *Chem. Soc. Rev.* **2018**, *47*, 8572−8610.

(3) Discher, B. M.; Won, Y.-Y.; Ege, D. S.; Lee, J. C-M.; Bates, F. S.; Discher, D. E.; Hammer, D. A. Polymersomes: Tough Vesicles Made from Diblock Copolymers. *Science* **1999**, *284*, 1143−1146.

(4) Discher, D. E.; Eisenberg, A. Polymer Vesicles. *Science* **2002**, *297*, 967−973.

(5) Pegoraro, C.; Cecchin, D.; Madsen, J.; Warren, N.; Armes, S. P.; MacNeil, S.; Lewis, A.; Battaglia, G. Translocation of flexible polymersomes across holes at the nanoscale. *Biomater. Sci.* **2014**, *2*, 680−692.

(6) Guo, X.; Szoka, F. C. Chemical Approaches to Triggerable Lipid Vesicles for Drug and Gene Delivery. *Acc. Chem. Res.* **2003**, *36*, 335−341.

(7) Joseph, A.; Contini, C.; Cecchin, D.; Nyberg, S.; Ruiz-Perez, L.; Gaitzsch, J.; Fullstone, G.; Tian, X.; Azizi, J.; Preston, J.; Volpe, G.; Battaglia, G. Chemotactic synthetic vesicles: Design and applications in blood-brain barrier crossing. *Sci. Adv.* **2017**, *3*, No. e1700362.

(8) Zhang, Z. F.; Xu, J.; Drapaca, C. Particle squeezing in narrow confinements. *Microfluid Nanofluidics* **2018**, *22*, 120.

(9) Plaks, V.; Koopman, C. D.; Werb, Z. Circulating tumor cells. *Science* **2013**, *341*, 1186−1188.

(10) Zhang, Z.; Xu, J.; Hong, B.; Chen, X. The effects of 3D channel geometry on CTC passing pressure—Towards deformability-based cancer cell separation. *Lab. Chip.* **2014**, *14*, 2576−2584.

(11) Paul, C. D.; Mistriotis, P.; Konstantopoulos, K. Cancer cell motility: Lessons from migration in confined spaces. *Nat. Rev. Cancer* **2017**, *17*, 131−140.

(12) Vormittag, P.; Gunn, R.; Ghorashian, S.; Veraitch, F. S. A guide to manufacturing CAR T cell therapies. *Curr. Opin. Biotechnol.* **2018**, *53*, 164−181.

(13) Gompper, G.; Kroll, D. M. Driven transport of fluid vesicles through narrow holes. *Phys. Rev. E* **1995**, *52*, 4198−4208.

(14) Tordeux, C.; Fournier, J.-B. Extravasation of adhering vesicles. *Europhys. Lett.* **2002**, *60*, 875−881.

(15) Ranguelov, B.; Milchev, A. Translocation kinetics of vesicles through narrow holes. *EPL* **2022**, *138*, 42001.

(16) Meng, F. L.; Chen, J. Z. Y.; Doi, M.; Ou-Yang, Z.-C. Phase diagrams and interface in inflating balloon. *AIChE J.* **2014**, *60*, 1393−1399.

(17) Han, Y.; Lin, H.; Ding, M.; Li, R.; Shi, T. Flow-induced translocation of vesicles through a narrow hole. *Soft Matter* **2019**, *15*, 3307−3314.

(18) Linke, G. T.; Lipowsky, R.; Gruhn, T. Osmotically induced passage of vesicles through narrow holes. *Europhys. Lett.* **2006**, *74*, 916−922.

(19) Shojaei, H. R.; Muthukumar, M. Translocation of an Incompressible Vesicle through a Pore. *J. Phys. Chem. B* **2016**, *120*, 6102−6109.

(20) Khunpetch, P.; Man, X. K.; Kawakatsu, T.; Doi, M. Translocation of a vesicle through a narrow hole across a membrane. *J. Chem. Phys.* **2018**, *148*, 134901.

(21) Kantor, Y.; Kardar, M.; Nelson, D. R. Statistical Mechanics of Tethered Surfaces. *Phys. Rev. Lett.* **1986**, *57*, 791−794.

(22) Doi, M. *Soft Matter Physics*; Oxford University Press: Oxford, U.K., 2013; pp 38−39, DOI: 10.1093/acprof:oso/9780199652952.001.0001.

(23) de Gennes, P.-G.; Brochard-Wyart, F.; Quéré, D. Capillarity: Deformable Interfaces. *Capillarity and Wetting Phenomena*; Springer: New York, 2004; pp 1−31, DOI: 10.1007/978-0-387-21656-0_1.

(24) Helfrich, W. Elastic Properties of Lipid Bilayers-Theory and Possible Experiments. *Z. Naturforsch. C* **1973**, *28*, 693−703.